



Influence of Estuarine Tidal Mixing on Structure and Spatial Scales of Large River Plumes

Alexander Osadchiev^{1,2}, Sergey Shchuka¹, Eduard Spivak³, Maria Pisareva¹, Igor Semiletov³

¹Shirshov Institute of Oceanology, Russian Academy of Sciences, Moscow, Russia

5 ²Institute of Geology of Ore Deposits, Petrography, Mineralogy and Geochemistry, Russian Academy of Sciences, Moscow, Russia

³Ilyichov Pacific Oceanological Institute, Far Eastern Branch of the Russian Academy of Sciences, Vladivostok, Russia

Correspondence to: Alexander Osadchiev (osadchiev@ocean.ru)

Abstract. The Yenisei and Khatanga rivers are among the largest estuarine rivers that inflow to the Arctic Ocean. Discharge
10 of the Yenisei River is one order of magnitude larger than that of the Khatanga River. However, spatial scales of buoyant
plumes formed by freshwater runoffs from the Yenisei and Khatanga gulfs are similar. This feature is caused by different
tidal forcing in these estuaries, which have similar sizes, climate conditions, and geomorphology. The Khatanga discharge
exhibits strong tidal forcing that causes formation of a diluted bottom-advected plume in the Khatanga Gulf. This
15 anomalously deep and weakly-stratified plume has a small freshwater fraction and, therefore, occupies a large area on the
shelf. The Yenisei Gulf, on the other hand, is a salt-wedge estuary that receives a large freshwater discharge and is less
affected by tidal mixing due to low tidal velocities. As a result, the low-salinity and strongly-stratified Yenisei plume has a
large freshwater fraction and its horizontal size is relatively small. The obtained results show that estuarine tidal mixing
determines freshwater fraction in these river plumes, which governs their depth and area after they spread from estuaries to
20 coastal sea. Therefore, influence of estuarine mixing on spatial scales of a large river plume can be of the same importance as
the roles of river discharge rate and wind forcing. In particular, rivers with similar discharge rates can form plumes with
significantly different areas, while plumes with similar areas can be formed by rivers with significantly different discharge
rates.

1 Introduction

River plumes play an important role in land-ocean interactions. Despite their relatively small volume as compared to
25 adjacent coastal seas, they significantly affect global fluxes of buoyancy, heat, terrigenous sediments, nutrients, and
anthropogenic pollutants, which are discharged to the coastal ocean with continental runoff [Dagg et al., 2004; Milliman and
Farnsworth, 2011; Lebreton et al., 2017; Schmidt et al., 2017]. As a result, dynamics and variability of river plumes are key
factors for understanding mechanisms of spreading, transformation, and redistribution of continental discharge and river-
borne constituents in coastal seas and their influence on adjacent continental shelves [Geyer et al., 2004; Hickey et al., 2010;
30 Hetland and Hsu, 2013]. World river plumes are characterized by wide variety of structure, morphology, and dynamical

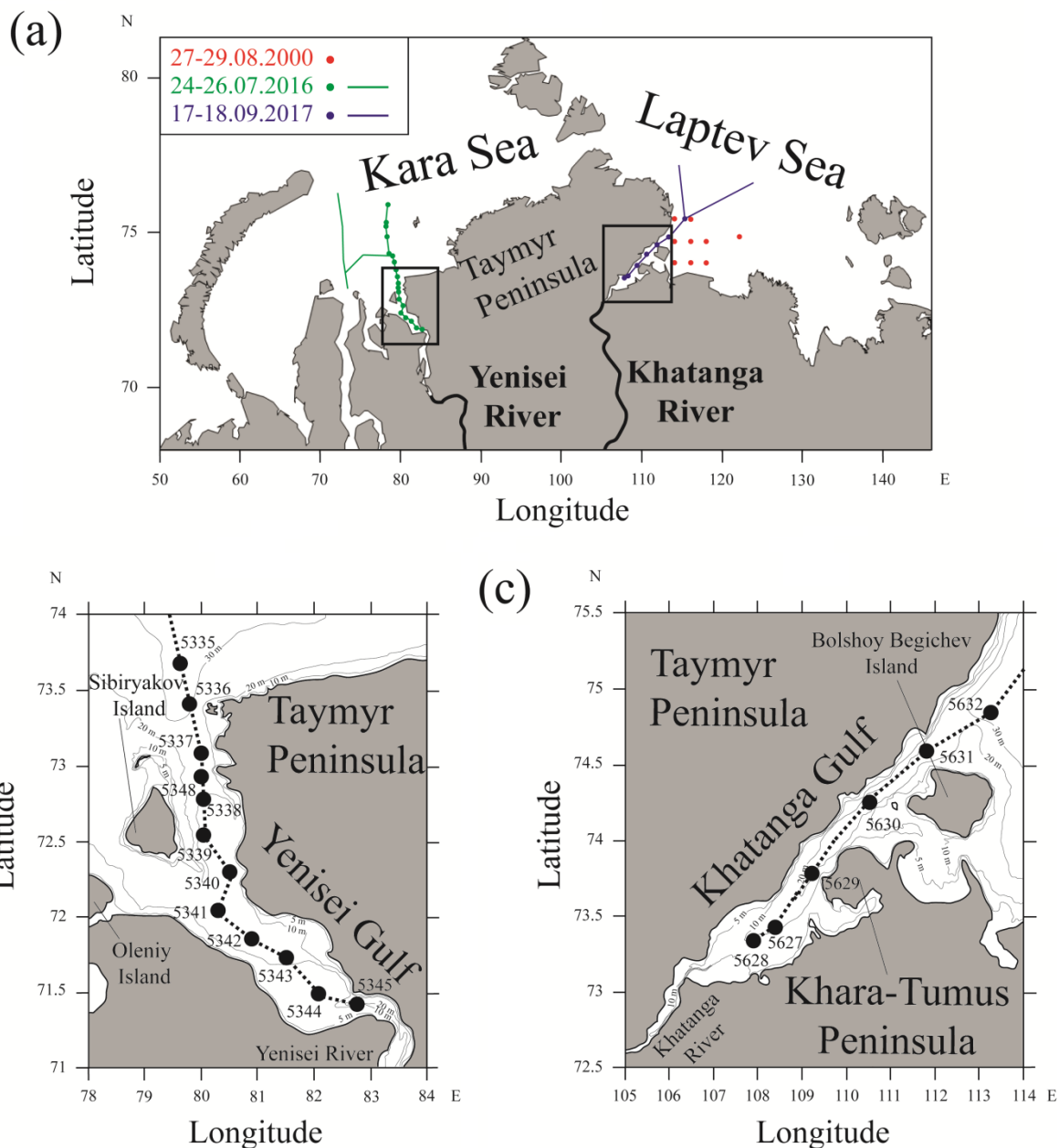


characteristics caused by large differences in regional features [Chant, 2011; Horner-Devine et al., 2015; Osadchiev and Korshenko, 2017], in particular, estuarine conditions [Guo and Valle-Levison, 2007; Nash et al., 2009; Lai et al., 2016]. River estuaries are areas where freshwater discharge initially interacts with saline sea water. The related processes of mixing of river runoff with sea water and formation of river plumes in estuaries determine their structure and govern their subsequent spreading and mixing in open sea. Intensity of estuarine mixing varies from negligible, when mostly undiluted freshwater discharge inflows directly to coastal sea, to dominant, which results in significant dilution of river discharge in well-mixed enclosed basins before being released to open sea [Schettini et al., 1998; Halverson and Palowicz, 2008; MacCready and Geyer, 2010; Geyer and MacCready, 2014].

The Yenisei and Khatanga estuaries are among the largest that flow into the Arctic Ocean. These Yenisei and Khatanga gulfs are closely located and have similar sizes, geomorphology, and climatic conditions, albeit significantly different tidal forcing. In this study we focus on transformation of discharge of the Yenisei and Khatanga rivers in their estuaries and spreading of their buoyant plumes that occupy wide areas in the Kara and Laptev seas. Discharge of the Yenisei River is one order of magnitude larger than of the Khatanga River. However, spatial scales of buoyant plumes formed by freshwater runoffs from the Yenisei and Khatanga gulfs are similar. Using in situ hydrographic data, we reveal that this feature is caused by difference in intensity of estuarine tidal mixing that greatly affects spatial scales of these river plumes.

2 Study area

Freshwater discharge of the Yenisei River (630 km³ annually) is the largest among Arctic rivers and accounts to 20% of total freshwater runoff to the Arctic Ocean [Gordeev et al., 1996; Carmack, 2000]. Hydrological regime of the Yenisei River is governed by a distinct freshet peak in June – July (half of total annual discharge), moderate discharge in May and August – September, and a drought in October – April [Pavlov et al., 1996; Guay et al., 2001]. The Yenisei River inflows into the Yenisei Gulf located at the southeastern part of the Kara Sea at the western side of the Taymyr Peninsula (Fig. 1). The Yenisei Gulf is 250 km long; its width is 35-50 km. Average depth of the southern (inner) part of the gulf increases off the river mouth from 5 to 15 m. The large Sibiryakov Island is located in northern (outer) part of the gulf and divides it into two 40-50 km long and 30-35 km wide straits (Fig. 1b). The western strait between the Sibiryakov and Oleniy islands is shallow (10 m deep), while depth of the eastern strait between the Sibiryakov Island and the Taymyr Peninsula steadily increases towards the open sea to 25-30 m and connects the Yenisei Gulf with the central part of the Kara Sea. The Yenisei Gulf is covered by ice in October – July. Tides are relatively low in the Yenisei Gulf, tidal amplitude and velocity do not exceed 0.5 m and 0.2 m/s [Kowalik and Proshutinsky, 1994; Padman and Erofeeva, 2004; Kagan et al., 2010, 2011].



60 **Figure 1: Study area; location of the Yenisei and Khatanga gulfs; ship tracks (lines) and location of hydrological stations (circles) of three oceanographic field surveys conducted in August 2000 (red) and September 2017 (blue) in the Laptev Sea and in July 2016 (green) in the Kara Sea (a). Bathymetry, ship tracks, and location of hydrological stations in the Yenisei (b) and Khatanga (c) gulfs.**

Freshwater discharge of the Khatanga River (105 km^3 annually) is much smaller than that of the Yenisei River.

65 Approximately one half of this volume is discharged to the Laptev Sea during freshet period in June, then the river discharge steadily decreases till September [Pavlov et al., 1996]. The lower part of the Khatanga River is completely frozen in October

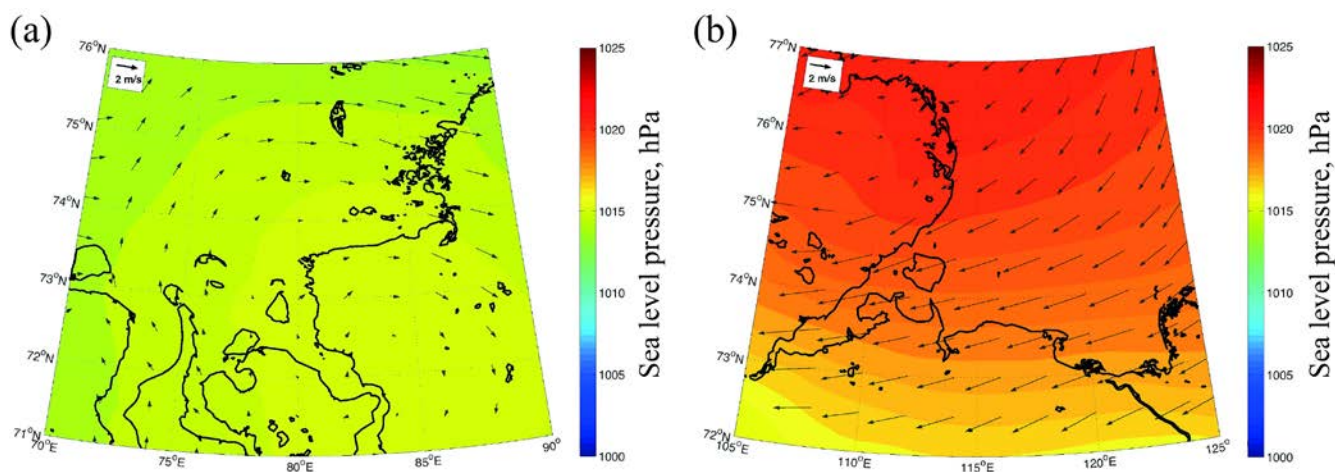


– May and during this period its discharge is negligible [Pavlov et al., 1996]. The Khatanga River inflows into the Khatanga Gulf which is located at the southwestern part of the Laptev Sea at the eastern side of the Taymyr Peninsula (Fig. 1). Shape, bathymetry, spatial scales, and climatic conditions of the Khatanga Gulf are similar to those of the Yenisei Gulf which is located approximately 800 km to the west from the Khatanga Gulf. The Khatanga Gulf is 250 km long; its width is 25-50 km. The shallow (5-20 m deep) inner and deep (20-30 m deep) outer parts of the gulf are connected by a narrow strait (15-20 km wide) between the Khara-Tumus and Taymyr peninsulas (Fig. 1c). The Bolshoy Begichev Island is located in the outer part of the Khatanga Gulf and divides it into two straits. The southern strait is narrow (8 km wide) and shallow (10 m deep), while depth of the northern strait (15-20 km wide) between the Bolshoy Begichev Island and the Taymyr Peninsula steadily increases towards the open sea to 25-30 m and connects the Khatanga Gulf with the western part of the Laptev Sea. The Khatanga Gulf is covered by ice in October – July. Tides in the Khatanga Gulf are among the largest in the Eurasian part of the Arctic Ocean. Maximal tidal range in different part of the gulf is 1-2 m [Pavlov et al., 1996; Kulikov et al., 2018]. The largest tidal velocities up to 1.4-1.7 m/s were registered at the straits that connect the outer part of the gulf with the inner part and the open sea, which are described above [Korovkin and Antonov, 1938; Pavlov et al., 1996].

3 Data

Hydrographic in situ data used in this study were collected during three oceanographic field surveys in the Kara and Laptev seas including the 4th cruise of the R/V “Nikolay Kolomeytssev” on 27-29 August 2000 in the south-western part of the Laptev Sea, the 66th cruise of the R/V “Akademik Mstislav Keldysh” on 24-26 July 2016 in the Yenisei Gulf and the central part of the Kara Sea, the 69th cruise of the R/V “Akademik Mstislav Keldysh” on 17-18 September 2017 in the Khatanga Gulf and the western part of the Laptev Sea (Fig. 1). Field surveys included continuous measurements of salinity in the surface sea layer (2-3 m depth) performed at 100 m spatial resolution along the ship track using a ship board pump-through system equipped by a conductivity-temperature-depth (CTD) instrument (*Sea-Bird Electronics SBE 21 SeaCAT Thermosalinograph*) [Zavialov et al., 2015; Osadchiev et al., 2017]. Vertical profiles of salinity were performed using a CTD instrument (*Sea-Bird Electronics SBE 911plus CTD*) at 0.2 m vertical resolution. This CTD profiler was equipped with two parallel temperature and conductivity sensors; the mean temperature differences between them did not exceed 0.01°C, while differences of salinity were not greater than 0.01. Discharge data used in this study was obtained at the most downstream gauge stations at the Yenisei and Khatanga rivers located approximately 650 and 200 km far from the river mouths, respectively.

The atmospheric influence on the Yenisei and Khatanga plumes was examined using 1 h ERA5 atmospheric reanalysis with a 0.25° resolution. Wind forcing during several weeks preceding in situ measurements in July 2016 in the Kara Sea and in September 2017 in the Laptev Sea was weak and moderate (Fig. 2). No storm events occurred during this period in the study areas, average wind speed was <4 m/s in the central part of the Kara Sea and <7 m/s in the western part of the Laptev Sea.



100 **Figure 2: Average wind forcing (arrows) and sea level pressure (color) during 12-26 July 2016 in the central part of the Kara Sea (a) and during 24-18 September 2017 in the western part of the Laptev Sea (b) obtained from ERA5 atmospheric reanalysis.**

4 Results

The in situ measurements performed in July 2016 in the Kara Sea during the period of peak discharge of the Yenisei River (approximately $30\,000\text{ m}^3/\text{s}$) revealed that the Yenisei plume was spreading more than 500 km northward from the river mouth and its depth and vertical structure did not change much along this distance (Fig. 3a). The Yenisei plume occupied the whole water column in the shallow inner part of the estuary, its surface salinity was 0-5 (stations 5341-5345). Further northward the plume detached from the sea bottom. The plume depth (defined by the isohaline of 25) remained equal to 8-12 m in the outer part of the estuary (stations 5337-5340) and at the Kara Sea shelf (stations 5336-5350). Surface salinity of the plume also was relatively stable and slowly increased from 6 to 10 in this 300 km long part of the transect. Sharp salinity gradient was observed between the plume and the subjacent sea, vertical distance between the isohalines of 10 and 25 did not exceed several meters. Further northward surface salinity abruptly increased from 15 (station 5351) to 28 (station 5352) in a distance of 10 km indicating the northern boundary of the Yenisei plume.

105
110

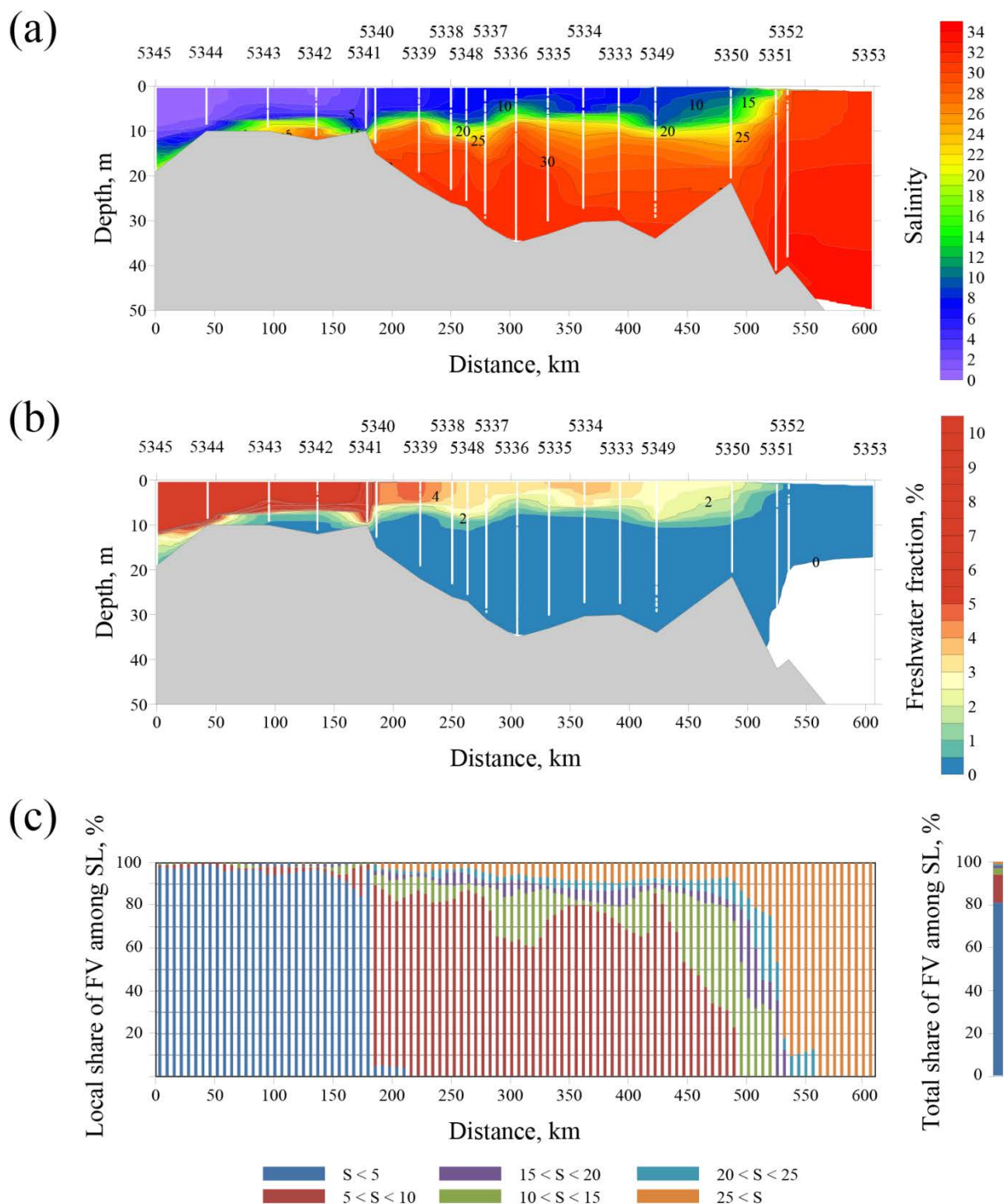
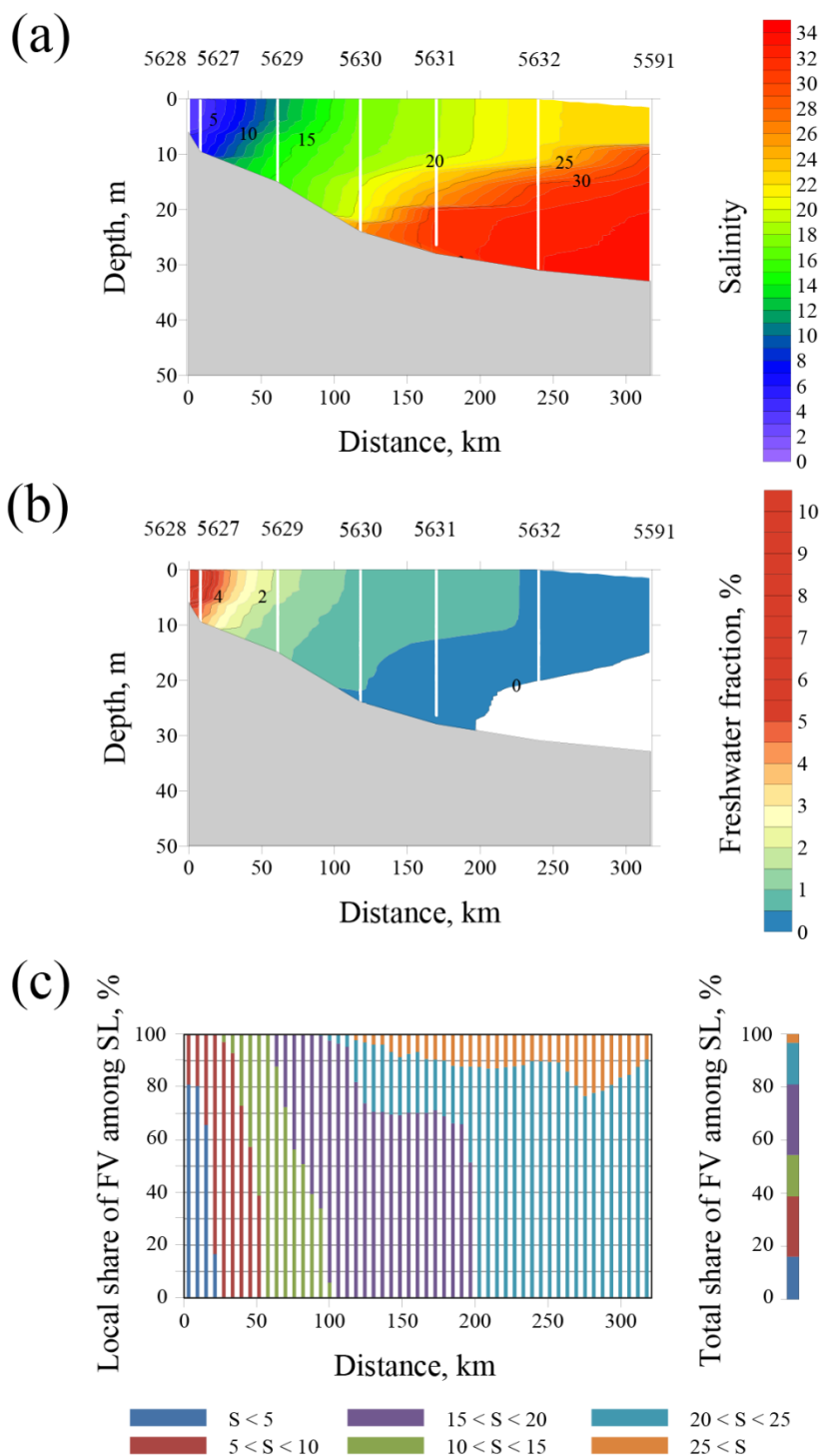


Figure 3: The vertical salinity structure (a), distribution of freshwater fraction (b), local and total shares of freshwater volume (FV) among salinity layers (SL) in water column (c) along the ship track in the Yenisei Gulf and the adjacent shelf of the Kara Sea on 24-26 July 2016.



According to Nash et al. [2009], to quantify the effect of estuarine mixing on the Yenisei plume we calculated vertical distribution of freshwater fraction $F = (S_0 - S) / S_0$ along the transect (Fig. 3b), where S is the observed salinity, S_0 is the reference ambient sea salinity prescribed equal to 32. F represents the volume fraction of freshwater in the Yenisei plume that produced the observed salinity after being mixed with ambient sea water. The value of the reference salinity equal to 32 was chosen according to typical salinity of ambient sea water at the shelves of the central part of the Kara Sea and southwestern part of the Laptev Sea [Pavlov et al., 1996; Johnson et al., 1997; Williams and Carmack, 2015] Figure 3 illustrates that the Yenisei discharge exhibited relatively little mixing in the estuary due to weak tidal forcing. As a result, the majority of river runoff propagated off the estuary within the low-saline and shallow Yenisei plume (Fig. 3b). Strong stratification between the plume and the subjacent shelf sea hindered vertical mixing. Freshwater fraction remained concentrated in the shallow and low-saline surface layer in the open part of the Kara Sea till station 5350 located 500 km far from the river mouth. The majority of freshwater volume in water column was located in two salinity layers, namely, between the isohalines of 0 and 5 (in the inner estuary) and between the isohalines of 5 and 10 (in the outer estuary and at sea shelf) (Fig. 3c). Salinity layers of 0-5 and 5-10 accounted for 80% and 15% of total freshwater volume along the transect, respectively (Fig. 3c).

Despite low discharge rate of the Khatanga River (approximately 3 000 m³/s) during 17-18 September 2017, the horizontal extent of the Khatanga plume was similar to that of the Yenisei plume, while its maximal depth even exceeded depth of the Yenisei plume (Fig. 4a). The Khatanga plume was weakly-stratified and occupied the whole water column in the shallow inner part of the estuary (stations 5627-2629) due to intense tidal mixing in the Khatanga Gulf. Tidal-induced dilution caused increase of surface salinity and depth of the plume from 4 and 7 m (station 5628) to 17 and 25 m (station 5630) at 120 km along the transect. In the outer part of the estuary the plume detached from sea bottom and its depth steadily decreased to 11 m, while surface salinity increased to 21 (station 5632). Further northeastward at the Laptev Sea shelf the plume salinity slightly increased to 22, while depth slightly decreased to 9 m in a distance of 100 km from the Khatanga Gulf (station 5591). Distinct salinity gradient between the plume and the subjacent sea was stable along the northeastern part of the transect. Vertical distance between the isohalines of 25 and 30 did not exceed several meters in the outer estuary and coastal sea. Salinity measurements performed in the surface layer revealed that the boundary of the Khatanga plume was located further northward, approximately 250 km from the Khatanga Gulf and 500 km far from the river mouth (Fig. 5c).



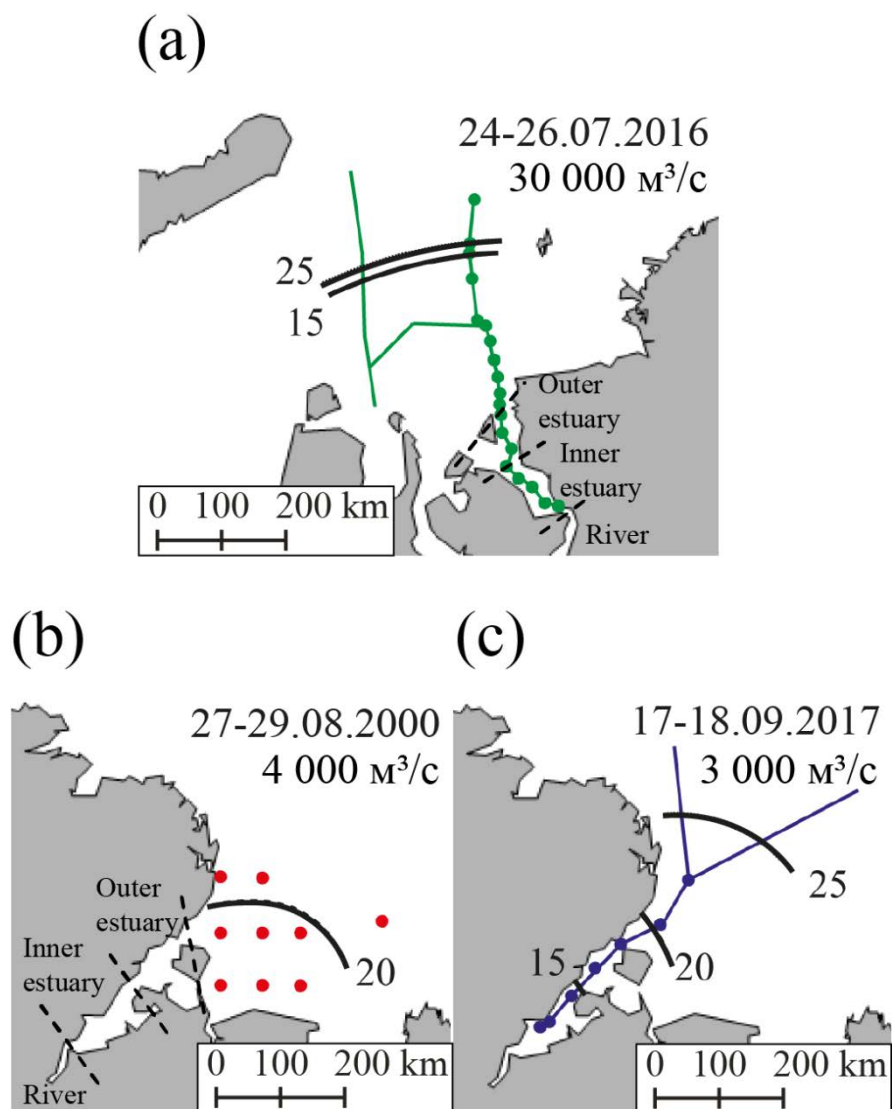
145 **Figure 4:** The vertical salinity structure (a), distribution of freshwater fraction (b), local and total shares of freshwater volume (FV) among salinity layers (SL) in water column (c) along the ship track in the Khatanga Gulf and the adjacent shelf of the Laptev Sea on 17-18 September 2017.



The Khatanga discharge exhibited intense estuarine tidal mixing and, therefore, was distributed from surface to bottom in the inner estuary and over 20-25 m deep water column in the outer estuary (Fig. 4b). As a result, relatively small freshwater volume formed a deep, but diluted river plume. Salinity and freshwater fraction in the Khatanga plume remained stable while it was spreading from the estuary to open part of the Laptev Sea. Freshwater volume in water column steadily transferred from salinity layer of 0-5 near the river mouth to salinity layer of 20-25 in the open sea (Fig. 4c). Total freshwater volume along the transect was almost homogeneously distributed among salinity layers of 0-5, 5-10, 10-15, 15-20, and 20-25 (Fig. 4c). Thus, the Khatanga plume was formed by relatively small volume of freshwater discharge, however, mixed with large volume of saline water in the estuary that is indicated by low freshwater fraction in the plume. As a result, the Khatanga plume occupied large volume and area at the Laptev Sea. In particular, surface salinity in the southwestern part of the Laptev Sea remained less than 25 at a distance of 250 km from the Khatanga Gulf (Fig. 5c).

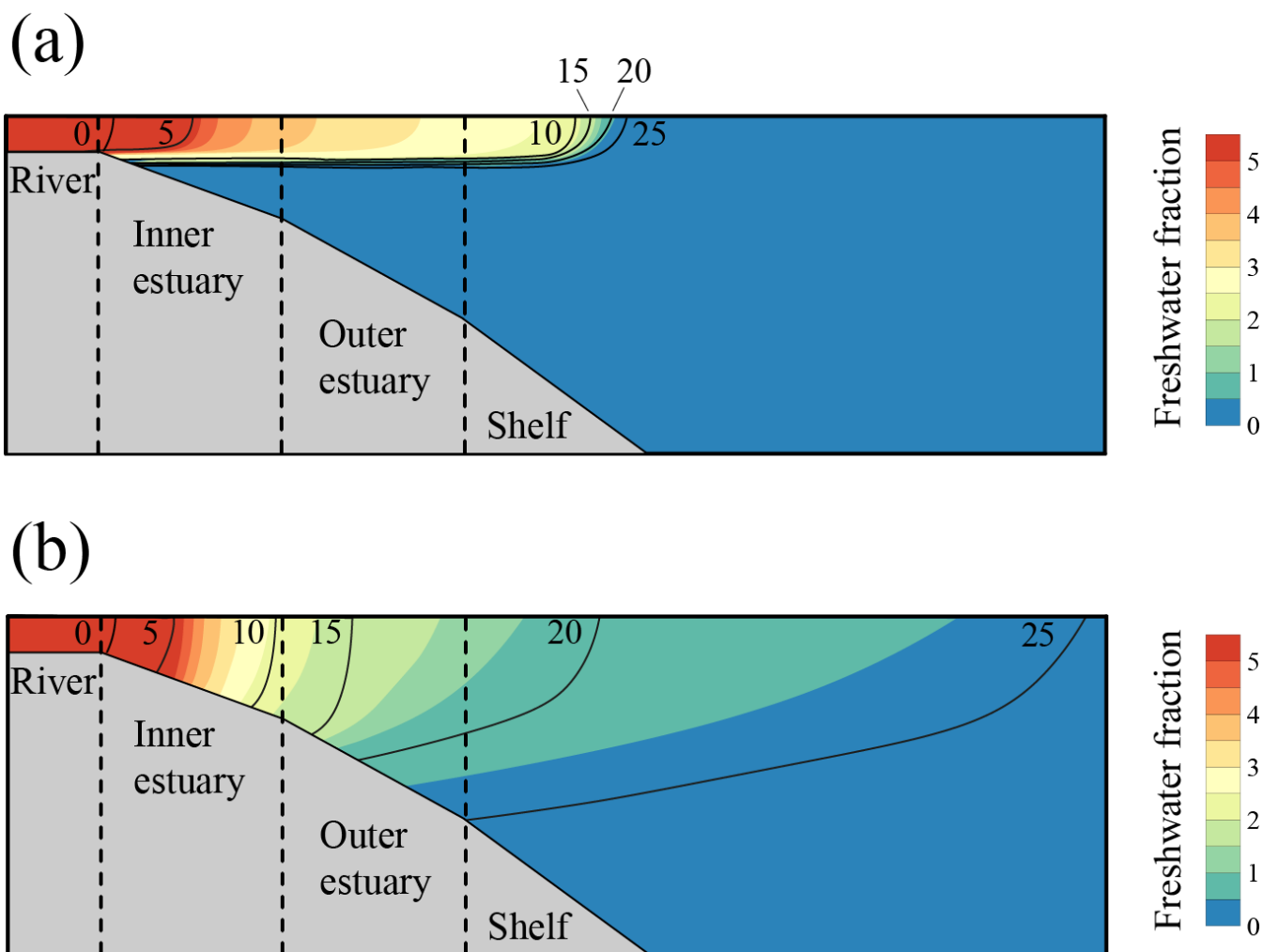
5 Discussion and Conclusions

River discharge rate, wind forcing, and tidal circulation are the main factors that determine estuarine circulation and govern vertical structure and spatial scales of river plumes [Nash et al., 2009; Horner-Devine et al., 2015]. In situ measurements performed in the Yenisei and Khatanga plumes described above revealed that spatial scales of these plumes were similar, while discharge rates of the Yenisei and Khatanga rivers differed by one order of magnitude. The Yenisei and Khatanga gulfs are closely located and have similar sizes, geomorphology, and climatic conditions, albeit significantly different tidal forcing. Wind conditions several weeks before and during the field sampling were moderate and low (Fig. 2), so the Yenisei and Khatanga plumes were only weakly affected by wind forcing during these periods. General shelf circulation also does not significantly impact buoyancy-driven and wind-driven spreading of the large Yenisei and Khatanga plumes [Guay et al., 2001; Panteleev et al., 2007; Zatsepin et al., 2010; Osadchiev et al., 2017; 2019]. Thus, we presume that similarity in spatial scales of these plumes is caused by difference in estuarine tidal mixing forcing that determined difference in their structure, in particular, different freshwater fractions. Freshwater fraction of a plume governs its spatial scales in a coastal sea, i.e., the same volume of freshwater can form a small freshened plume with large freshwater fraction (Fig. 6a) or a large diluted plume with small freshwater fraction (Fig. 6b). Thus, rivers with similar discharge rates can form plumes with significantly different areas. This result is in a good agreement with Fischer [1972] and Nash [2009], that showed that vertical structure and stratification of a buoyant plume is governed by both river discharge and tidal velocities. On the other hand, plumes with similar areas can be formed by rivers with significantly different discharge rates. The latter situation is the case of the Yenisei and Khatanga plumes (Fig. 5).



175

Figure 5: Location of isohalines of 15, 20, and 25 (black lines) at the central part of the Kara Sea (a) and the western part of the Laptev Sea (b, c) indicating spatial scales of the Yenisei (a) and Khatanga (b, c) river plumes reconstructed from in situ measurements conducted in August 2000 (red) and September 2017 (blue) in the Laptev Sea and in July 2016 (green) in the Kara Sea.



180

Figure 6: Schematics of vertical distribution of freshwater fraction for river plumes formed by the same volume of freshwater discharge in estuaries with low (a) and high (b) mixing forcing.

The vertical in situ measurements performed along the transects in combination with continuous salinity measurements in the surface layer along the ship track detected location of the northern plume borders defined by the isohaline of 25 (Fig. 5a, 185 5c). On the other hand, eastern and western segments of the plume borders and, therefore, the zonal extents of the plumes were not directly detected by in situ measurements. Nevertheless, the obtained data are representative of the total surface areas of the Yenisei and Khatanga plumes due to the following reasons. Unlike small and medium-size river plumes, in which alongshore and cross-shore extents can be significantly different [Yankovsky and Chapman, 1997; Fong and Geyer, 2002; Chant, 2011; Korotenko et al., 2014; Osadchiev and Sedakov, 2019], plumes formed by large rivers generally have similar zonal and meridional extents, e.g., the Amazon plume [Lentz and Limeburner, 1995; Geyer et al., 1996], the Congo plume [Denamiel et al., 2013], the Yangtze plume [Yuan et al., 2016], the Orinoco plume [Del Castillo et al., 1999], the Mississippi plume [Schiller et al., 2011]. This is also the case of the large Yenisei and Khatanga plumes formed in the semi- 190



isolated central part of the Kara Sea and western part of the Laptev Sea [Pavlov et al., 1996; Zatsepin et al., 2010; Zavalov et al., 2015]. As a result, the transects that cross the plumes from their sources in the estuaries through central parts of the plumes to their offshore parts are sufficient to quantify similarity of areas of the Yenisei and Khatanga plumes.

195 Large freshwater discharge of the Yenisei River estimated as 30000 m³/s did not exhibit intense mixing in the estuary and formed a relatively shallow (8-12 m), low-salinity, strongly-stratified plume (Fig. 3a). In situ measurements along the ship track showed that northern boundary of the Yenisei plume was located 250 km from the Yenisei Gulf (Fig. 5a). On the other hand, moderate discharge of the Khatanga River estimated as 3000 m³/s formed anomalously deep (15-25 m), but diluted

200 and weakly stratified plume in the middle of September 2017 (Fig. 4a). In situ measurements along the ship track showed that surface salinity in the southwestern part of the Laptev Sea estimating remained less than 25 at a distance of 200-250 km from the Khatanga Gulf (Fig. 5c). Another field survey conducted at the southwestern part of the Laptev Sea in the end of August 2000 also showed that the Khatanga plume occupied a large area (Fig. 5b). Distinct location of plume boundaries was not detected during this field survey due to absence of continuous measurements of surface salinity along the ship track.

205 However, vertical profiles of salinity obtained at hydrological stations showed that isohaline of 20 in the surface layer was located 50-200 km from the Khatanga Gulf. It indicates that area of the Khatanga plume formed by moderate discharge (approximately 4000 m³/s in August 2000 and 3000 m³/s in September 2017) of the Khatanga River was of the same order as area of the Yenisei plume in July 2016 formed by large discharge (approximately 30000 m³/s) of the Yenisei River.

This result is supported by vertical distributions of freshwater volume among salinity layers in the Yenisei (Fig. 3c) and

210 Khatanga (Fig. 4c) plumes. The majority of freshwater volume contained in the Yenisei plume in the inner estuary was located in 0-5 salinity layer. After the plume propagated to the outer estuary, this freshwater volume transferred to 5-10 salinity layer and stably remained in this layer, when the plume was spreading over the open sea. As a result, 95% of freshwater discharge of the Yenisei River was mixed with a relatively small volume of saline sea water and formed 0-5 and 5-10 salinity layers within the Yenisei plume with relatively small volumes. On the other hand, freshwater volume contained

215 in the Khatanga plume steadily transferred from 0-5 salinity layer near the river mouth to 20-25 salinity layer in the outer estuary and sea shelf. Thus, freshwater discharge of the Khatanga River was diluted by a large volume of saline sea water in the estuary and formed the 20-25 saline Khatanga plume with relatively large volume. This plume was spreading outside the estuary and covered wide area in the southwestern part of the Laptev Sea. Thus, intense estuarine tidal mixing caused formation of an anomalously deep and large Khatanga plume from relatively small discharge of the Khatanga River.

220 Based on the reconstructed vertical distributions of freshwater fraction along the transects in the Yenisei and Khatanga plumes, for both transects we calculated the related transect freshwater “volumes” $T = \int_0^L \left(\int_{-h(x)}^0 F(x, z) dz \right) dx$, where x and z are the horizontal (along a transect) and vertical coordinates, respectively, $F(x, z)$ is the freshwater fraction at the point (x, z) , $h(x)$ is the sea depth, L is the length of the transect. The resulting transect freshwater “volumes” of the Yenisei and Khatanga plumes, namely, T_Y and T_K , are two-dimensional. i.e., they do not consider lateral dimensions of the river plumes. However,

225 their ratio is indicative of ratio of freshwater volumes, which are contained within these river plumes, due to similar form



and sizes of the Yenisei and Khatanga gulfs. Actually, $T_Y / T_K = 46 / 5 = 9.3$ that is close to ratio between discharge rates of the Yenisei and Khatanga rivers during the periods of field measurements $Q_Y / Q_K = 30000 / 3000 = 10$. This good agreement proves that the reconstructed distributions of freshwater fraction along the transects indeed represent distributions of volumes of freshwater discharge of the Yenisei and Khatanga rivers that formed the river plumes after being mixed with saline sea water.

230 A number of previous works stated that river discharge rate and wind forcing are the main external conditions that govern size of a river plume [Whitney and Garvine, 2005; O'Donnell et al., 2008; Chant, 2011; Osadchiev and Zavialov, 2013; Horner-Devine et al., 2015]. In this study we show that influence of estuarine mixing on spatial scales of a large river plume in a coastal sea can be of the same importance as the roles of river discharge rate and wind forcing. The obtained results allow getting new insights into the processes of spreading and transformation of river discharge in coastal sea. This issue is especially important for the Arctic Ocean that receives more than three-quarters of total freshwater runoff from ten large rivers [Gordeev et al., 1996; Carmack, 2000; Guay et al., 2001]. Moreover, during freshet periods in June – July the majority of annual freshwater discharge of large Arctic rivers flows into coastal areas which are mostly covered by ice. As a result, formation and spreading of these large river plumes is only weakly affected by wind forcing during these periods. Thus, study of estuarine and deltaic mixing conditions that determine spatial scales and structure of large Arctic river plumes is essential for assessment of large-scale freshwater transport in the Arctic Ocean which plays a key role in stratification and ice formation, as well as in many physical, biochemical, and geological processes [Carmack et al., 2010; Nummelin et al., 2016].

Competing interests

245 The authors declare that they have no conflict of interest.

Acknowledgments

This research was funded by the Ministry of Science and Education of Russia, theme 0149-2019-0003 (collecting of in situ data); the Russian Foundation for Basic Research, research projects 18-05-60302 (processing of in situ data), 18-05-60069 (analysis of atmospheric reanalysis data), 20-35-70039 (analysis of in situ data), and 18-05-00019 (study of river plumes); the Russian Science Foundation, research project 18-17-00089 (collecting of river discharge data); the Grant of the President of the Russian Federation for state support of young Russian scientists – candidates of science, research project MK-98.2020.5 (study of freshwater transport). The river discharge data were downloaded from the repository of the Federal Service for Hydrometeorology and Environmental Monitoring of Russia <http://gis.vodinfo.ru/> (available after registration). The ERA5 reanalysis data were downloaded from the European Centre for Medium-Range Weather Forecasts (ECMWF) website <https://www.ecmwf.int/en/forecasts/datasets/archive-datasets/reanalysis-datasets/era5>.



References

- Carmack, E. C.: The freshwater budget of the Arctic Ocean: Sources, storage and sinks. In: The freshwater budget of the Arctic Ocean. E.L. Lewis, E.P. Jones (Eds.), Kluwer, Dordrecht, Netherlands, pp. 91–126, 2000.
- Carmack, E. C., Yamamoto-Kawai, M., Haine, T. W., Bacon, S., Bluhm, B. A., Lique, C., Melling, H., Polyakov, I. V.,
260 Straneo, F., Timmermans, M.-L., and Williams, W. J.: Freshwater and its role in the Arctic Marine System: Sources, disposition, storage, export, and physical and biogeochemical consequences in the Arctic and global oceans, *J. Geophys. Res. Biogeosciences*, 121, 675–717, doi:10.1002/2015JG003140, 2016.
- Chant, R. J.: Interactions between estuaries and coasts: river plumes—their formation transport and dispersal. In: *Treatise on Estuarine and Coastal Science*. Vol. 2. E. Wolanski, D. McLusky (Eds.), Elsevier, Amsterdam, Netherlands, pp. 213–235,
265 2011.
- Dagg, M., Benner, R., Lohrenz, S., and Lawrence, D.: Transformation of dissolved and particulate materials on continental shelves influenced by large rivers: plume processes, *Cont. Shelf Res.*, 24, 833–858, doi:10.1016/j.csr.2004.02.003, 2004.
- Del Castillo, C. E., Coble, P. G., Morell, J. M., Lopez, J. M., and Corredor, J. E.: Analysis of the optical properties of the Orinoco River plume by absorption and fluorescence spectroscopy, *Mar. Chem.*, 66, 35–51, doi:10.1016/s0304-
270 4203(99)00023-7, 1999.
- Denamiel, C., Budgell, W. P., and Toumi, R.: The Congo River plume: Impact of the forcing on the far-field and near-field dynamics, *J. Geophys. Res.*, 118, 964–989, doi:10.1002/jgrc.20062, 2013.
- Fischer, H. B.: Mass transport mechanisms in partially stratified estuaries, *J. Fluid. Mech.*, 53, 671–687, doi:10.1017/S0022112072000412, 1972.
- 275 Fong, D. A. and Geyer, W. R.: The alongshore transport of freshwater in a surface-trapped river plume, *J. Phys. Oceanogr.*, 32, 957–972, doi:10.1175/1520-0485(2002)032<0957:TATOFI>2.0.CO;2, 2002.
- Geyer W. R., Beardsley, R. C., Lentz, S. J., Candela, J., Limeburner, R., Johns, W. E., Castro, B. M., and Soares, I. D.: Physical oceanography of the Amazon shelf, *Cont. Shelf Res.*, 16, 575–616, doi:10.1016/0278-4343(95)00051-8, 1996.
- Geyer, W. R., Hill, P. S., and Kineke, G. C.: The transport, transformation and dispersal of sediment by buoyant coastal
280 flows, *Cont. Shelf Res.*, 24, 927–949, doi:10.1016/j.csr.2004.02.006, 2004.
- Geyer, W. R. and MacCready, P.: The estuarine circulation, *Annu. Rev. Fluid Mech.*, 46, 175–197, doi:10.1146/annurev-fluid-010313-141302, 2014.
- Gordeev, V. V., Martin, J. M., Sidorov, J. S., and Sidorova, M. V.: A reassessment of the Eurasian river input of water, sediment, major elements, and nutrients to the Arctic Ocean, *Am. J. Sci.*, 296, 664–691, doi:10.2475/ajs.296.6.664, 1996.
- 285 Guay, C. K., Falkner, K. K., Muench, R. D., Mensch, M., Frank, M., and Bayer, R.: Wind-driven transport pathways for Eurasian Arctic river discharge, *J. Geophys. Res.*, 106, C6, 11469–11480, doi:10.1029/2000JC000261, 2001.
- Guo, X. and Valle-Levinson, A.: Tidal effects on estuarine circulation and outflow plume in the Chesapeake Bay, *Cont. Shelf Res.*, 27, 20–42, doi:10.1016/j.csr.2006.08.009, 2007.



- Halverson, M. J. and Palowicz, R.: Estuarine forcing of a river plume by river flow and tides, *J. Geophys. Res.*, 113, C09033, doi:10.1029/2008JC004844, 2008.
- Hetland, R. D. and Hsu, T.-J.: Freshwater and sediment dispersal in large river plumes. In: *Biogeochemical Dynamics at Large River-Coastal Interfaces: Linkages with Global Climate Change*. T. S. Bianchi, M. A. Allison, W.-J. Cai (Eds.), Springer, New York, USA, pp. 55–85, 2013.
- Hickey, B. M., Kudela, R. M., Nash, J. D., Bruland, K. W., Peterson, W. T., MacCready, P., Lessard, E. J., Jay, D. A., Banas, N. S., Baptista, A. M., Dever, E. P., Kosro, P. M., Kilcher, L. K., Horner-Devine, A. R., Zaron, E. D., McCabe, R. M., Peterson, J. O., Orton, P. M., Pan, J., and Lohan, M. C.: River influences on shelf ecosystems: introduction and synthesis. *J. Geophys. Res.*, 115, C00B17, doi: 10.1029/2009JC005452, 2010.
- Horner-Devine, A. R., Hetland, R. D., and MacDonald, D. G.: Mixing and transport in coastal river plumes, *Annu. Rev. Fluid Mech.*, 47, 569–594, doi:10.1146/annurev-fluid-010313-141408, 2015.
- Johnson, D. R., McClimans, T. A., King, S., and Grenness, O.: Fresh water masses in the Kara Sea during summer, *J. Mar. Sys.*, 12, 127–145, doi:10.1016/S0924-7963(96)00093-0, 1997.
- Kagan, B. A., Timofeev, A. A., and Sofina, E. V.: Seasonal variability of surface and internal M2 tides in the Arctic Ocean, *Izv. Atmos. Ocean. Phys.*, 46, 652–662, doi:10.1134/S0001433810050105, 2010.
- Kagan, B. A., Sofina, E. V., and Timofeev, A. A.: Modeling of the M2 surface and internal tides and their seasonal variability in the Arctic Ocean: Dynamics, energetics and tidally induced diapycnal diffusion, *J. Mar. Res.*, 69, 245–276, doi:10.1357/002224011798765312, 2011.
- Korotenko, K. A., Osadchiv, A. A., Zavialov, P. O., Kao, R.-C., and Ding, C.-F.: Effects of bottom topography on dynamics of river discharges in tidal regions: case study of twin plumes in Taiwan Strait, *Ocean Sci.*, 10, 865–879, doi: 10.5194/os-10-863-2014, 2014.
- Korovkin, I. P. and Antonov, V. S.: Tides in the Khatanga River and the Khatanga Bay. *Proceedings of the All-Union Scientific Research Institute*, 105, 125–141, 1938. [in Russian]
- Kulikov, M. E., Medvedev, I. P., and Kondrin, A. T.: Seasonal variability of tides in the Arctic seas, *Russ. J. Earth Sci.*, 18, ES5003, doi:10.2205/2018ES000, 2018.
- Lai, Z., Ma, R., Huang, M., Chen, C., Chen, Y., Xie, C., and Beardsley, R. C.: Downwelling wind, tides, and estuarine plume dynamics, *J. Geophys. Res. Oceans*, 121, 4245–4263, doi:10.1002/2015JC011475, 2016.
- Lebreton, L.C., Zwet, J., Damsteeg, J. W., Slat, B., Andrady, A., Reisser, J.: River plastic emissions to the world’s oceans, *Nat. Commun.*, 8, 15611, doi:10.1038/ncomms15611, 2017.
- Lentz, S. J. and Limeburner, R.: The Amazon River Plume during AMASSEDS: Spatial characteristics and salinity variability, *J. Geophys. Res. Oceans*, 100, 2355–2375, doi:10.1029/94jc01411, 1995.
- MacCready, P. and Geyer, W. R.: Advances in estuarine physics, *Annu. Rev. Mar. Sci.*, 2, 35–58, doi:10.1146/annurev-marine-120308-081015, 2010.



- Milliman, J. D. and Farnsworth, K. L.: River Discharge to the Coastal Ocean: A Global Synthesis. Cambridge University Press, Cambridge, UK, doi:0.1017/CBO9780511781247, 2011.
- Nash, J. D., Kilcher, L. F., and Moum, J. N.: Structure and composition of a strongly stratified, tidally pulsed river plume, *J. Geophys. Res.*, 114, C00B12, doi:10.1029/2008JC005036, 2009.
- 325 Nummelin, A., Ilicak, M., Li, C., and Smedsrud, L. H.: Consequences of future increased Arctic runoff on Arctic Ocean stratification, circulation, and sea ice cover, *J. Geophys. Res. Oceans*, 121, 617–637, doi:10.1002/2015JC011156, 2016.
- O’Donnell, J., Ackleson, S. G., and Levine, E. R.: On the spatial scales of a river plume, *J. Geophys. Res.*, 113, C04017, doi:10.1029/2007JC004440, 2008.
- 330 Osadchiev, A.A., Asadulin, En.E., Miroshnikov, A.Yu., Zavialov, I.B., Dubinina, E.O., Belyakova, P.A.: Bottom sediments reveal inter-annual variability of interaction between the Ob and Yenisei plumes in the Kara Sea, *Sci. Rep.*, 9, 18642, doi:10.1038/s41598-019-55242-3, 2019.
- Osadchiev, A. A., Izhitskiy, A. S., Zavialov, P. O., Kremenetskiy, V. V., Polukhin, A. A., Pelevin, V. V., and Toktamysova, Z. M.: Structure of the buoyant plume formed by Ob and Yenisei river discharge in the southern part of the Kara Sea during
335 summer and autumn, *J. Geophys. Res. Oceans*, 122, 5916–5935, doi:10.1002/2016JC012603, 2017.
- Osadchiev, A. and Korshenko, E.: Small river plumes off the northeastern coast of the Black Sea under average climatic and flooding discharge conditions, *Ocean Sci.*, 13, 465–482, doi:10.5194/os-13-465-2017, 2017.
- Osadchiev, A.A. and Sedakov, R.O.: Spreading dynamics of small river plumes off the northeastern coast of the Black Sea observed by Landsat 8 and Sentinel-2, *Rem. Sens. Environ.*, 221, 522–533, doi:10.1016/j.rse.2018.11.043, 2019.
- 340 Osadchiev A. and Zavialov, P.: Lagrangian model of a surface-advected river plume, *Cont. Shelf Res.*, 58, 96–106, doi:10.1016/j.csr.2013.03.010, 2013.
- Padman, L. and Erofeeva, S.: A barotropic inverse tidal model for the Arctic Ocean. *Geophys. Res. Lett.*, 31, L02303, doi:10.1029/2003GL019003, 2004.
- Panteleev, G., Proshutinsky, A., Kulakov, M., Nechaev, D. A., and Maslowski W.: Investigation of the summer Kara Sea
345 circulation employing a variational data assimilation technique, *J. Geophys. Res.*, 112, C04S15, doi:10.1029/2006JC003728, 2007.
- Pavlov, V. K., Timokhov, L. A., Baskakov, G. A., Kulakov, M. Y., Kurazhov, V. K., Pavlov, P. V., Pivovarov, S. V., and Stanovoy, V. V.: Hydrometeorological regime of the Kara, Laptev, and East-Siberian seas. Technical Memorandum, APL-UW TM 1-96, Applied Physics Laboratory, University of Washington, 1996.
- 350 Schettini, C. A. F., Kuroshima, K. N., Fo, J. P., Rorig, L. R., and Resgalla Jr., C.: Oceanographic and ecological aspects of the Itajai-acu River plume during a high discharge period, *An. Acad. Bras. Ci.*, 70, 335–352, 1998.
- Schiller, R. V., Kourafalou, V. H., Hogan, P., Walker, N. D.: The dynamics of the Mississippi River plume: Impact of topography, wind and offshore forcing on the fate of plume waters, *J. Geophys. Res. Oceans*, 116, C6, doi:10.1029/2010jc006883, 2011.



- 355 Schmidt, C., Krauth, T., and Wagner, S.: Export of plastic debris by rivers into the sea, *Environ. Sci. Technol.*, 51, 21, 12246–12253, doi:10.1021/acs.est.7b02368, 2017.
- Williams, W. J. and Carmack, E. C.: The ‘interior’ shelves of the Arctic Ocean: Physical oceanographic setting, climatology and effects of sea-ice retreat on cross-shelf exchange, *Prog. Oceanogr.*, 139, 24–31, doi:10.1016/j.pocean.2015.07.008, 2015.
- Whitney, M. M. and Garvine, R. W.: Wind influence on a coastal buoyant outflow, *J. Geophys. Res.*, 110, C03014, 360 doi:10.1029/2003jc002261, 2005.
- Yankovsky, A. E. and Chapman, D. C.: A simple theory for the fate of buoyant coastal discharges, *J. Phys. Oceanogr.*, 27, 1386–1401, doi:10.1175/1520-0485(1997)027<1386:astftf>2.0.co;2, 1997.
- Yuan, R., Wu, H., Zhu, J., and Li, L.: The response time of the Changjiang plume to river discharge in summer, *J. Mar. Syst.*, 154, 82–92, doi:10.1016/j.jmarsys.2015.04.001, 2016.
- 365 Zatsepin, A. G., Zavialov, P. O., Kremenetskiy, V. V., Poyarkov, S. G., and Soloviev, D. M.: The upper desalinated layer in the Kara Sea, *Oceanology*, 50, 657–667, doi:10.1134/s0001437010050036, 2010.
- Zavialov, P. O., Izhitskiy, A. S., Osadchiev, A. A., Pelevin, V. V., and Grabovskiy, A. B.: The structure of thermohaline and bio-optical fields in the upper layer of the Kara Sea in September 2011, *Oceanology*, 55, 461–471, doi:10.1134/s0001437015040177, 2015.